

Structural and magnetization density studies of La_2NiO_4

G. H. Lander

Commission of European Communities, Joint Research Centre, Postfach 2340, D-7500 Karlsruhe, Federal Republic of Germany

P. J. Brown

Institut Laue-Langevin 156X, 38042 Grenoble CEDEX, France

J. Spáček and J. M. Honig

Department of Physics and Department of Chemistry, Purdue University, West Lafayette, Indiana 47907-3699

(Received 8 May 1989)

Neutron diffraction experiments have been performed on single crystals of La_2NiO_4 . Above 70 K the structure is orthorhombic $Bmab$. At 70 K a first-order transition occurs to a crystal structure that we believe to be tetragonal $P4_2/ncm$. With our resolution we see no splitting of the diffraction peaks that would indicate the lower-symmetry orthorhombic $Pccn$. A crystallographic refinement of 307 independent reflections from two different crystals gives an R factor of 6% for the $P4_2/ncm$ phase. The refinement also shows that our crystals are stoichiometric with an oxygen composition of 4.02 ± 0.03 . The crystals are antiferromagnetic with a magnetic structure in which the propagation and spin directions are parallel to $[100]$, in agreement with other studies. The antiferromagnetic ordered moment at $T = 10$ K is $(1.62 \pm 0.05)\mu_B$ per Ni atom. According to susceptibility measurements $T_N \approx 650$ K on stoichiometric La_2NiO_4 , but we have not checked this in our neutron experiment. No change in the antiferromagnetic structure occurs at the 70-K transition, but we cannot exclude the formation of a $2k$ magnetic structure at this temperature that would give rise to the same diffraction pattern in the tetragonal phase. In the second part of our experiment the induced magnetic form factor ($H = 4.6$ T, applied parallel to the $[010]$ axis at 5 K) has been measured with polarized neutrons. Our object in this experiment was to search for covalency effects, in particular evidence of interaction between the Ni $d_{x^2-y^2}$ orbital and the p_x, p_y orbitals of the oxygens in the Ni-O plane. We have measured 18 reflections with three different neutron wavelengths. The induced moment is $7.9 m\mu_B$ per molecule, which is in good agreement with bulk susceptibility measurements. Surprisingly, we find *no* evidence for any spin transfer or asphericity in the Ni spin density in the Ni-O planes. Instead we find new effects along the long c axis. The La^{3+} atoms develop a positive susceptibility which we suggest comes from hybridization between the La $5d$ and O p bands.

I. INTRODUCTION

Soon after the discovery¹ of superconductivity in doped La_2CuO_4 , neutron-diffraction experiments were undertaken on polycrystalline material to obtain the structural parameters, and especially the positions of the oxygen atoms and overall stoichiometry.² More recently, the results of neutron studies of single crystals have been reported,³ confirming the space-group assignment at low-temperature given by the powder work. These have also led to a better understanding of the "twinning" arrangement that occurs when the high-temperature tetragonal (HTT) with space-group $I4/mmm$ distorts (at 533 K in La_2CuO_4) to low-temperature orthorhombic (LTO) with space-group $Bmab$. (We follow the convention throughout this paper that the long c axis of the HTT cell remains the c axis of the LTO cell. This is consistent with Ref. 3, but different from Ref. 2.)

La_2NiO_4 is isostructural with La_2CuO_4 and also exhibits a structural distortion to orthorhombic symmetry at ~ 700 K in stoichiometric samples.⁴ However,

Rodriguez-Carvajal *et al.*⁵ reported a further transition at ~ 80 K in polycrystalline material in which the strain (related to the difference in length between the a and b orthorhombic axes) suddenly reduces in magnitude. One of our objectives was to study this lower-temperature transition with single crystals.

Our main objective, however, was to measure the *induced* magnetization density in La_2NiO_4 and compare it with measurements that were already in progress, since reported,⁶ on La_2CuO_4 . These measurements can, in principle, give information on the covalency between the metal $3d$ states and the oxygen p electrons; a subject of considerable importance in many of the theories addressing high- T_c superconductivity in layered copper-oxide materials. As we shall see, this comparison between the Cu and Ni compounds is more complicated than anticipated. More recently, superconductivity has been reported⁷ in Sr-doped La_2NiO_4 , so this greatly increases the interest in studies of the parent Ni compound. Under the right cycling conditions, diamagnetism has also been reported⁸ in La_2NiO_4 itself.

II. CRYSTAL PREPARATION

Single crystals of $\text{La}_2\text{NiO}_{4+\delta}$ were prepared by a crucibleless technique involving operation of a skull melter as described in Ref. 9. Appropriate amounts of La_2O_3 and NiO were prereacted to form the polycrystalline compound; the prereacted mixture was reground and fired for 24–36 h at 1200°C in a nickel crucible several times before loading the skull melter. After melting almost the entire 1-kg mass in the rf field, the boule was gradually cooled to room temperature. A single crystal was removed, oriented, cut, and reannealed at 1000°C under a controlled oxygen pressure $P_{\text{O}_2} = 10^{-11.5}$ atm in a $\text{CO}_2\text{-CO}$ buffering atmosphere. The sample was quenched and the surface layers removed by abrasion. The above procedure produced a single-crystal specimen of uniform oxygen composition with $\delta = 0.001\text{--}0.002$.

III. STRUCTURAL STUDIES

A. Data collection

Neutron experiments were performed on two single crystals of dimensions ~ 60 and 20 mm^3 . The first crystal was oriented with a short b axis almost vertical and the second crystal with the c axis approximately vertical. Integrated intensities were collected with the $D15$ normal-beam diffractometer at the High-Flux Reactor at the Institut Laue-Langevin (ILL), Grenoble. The neutrons ($\lambda = 1.76\text{ \AA}$) were obtained with a $\text{Cu}(220)$ monochromator and the $\lambda/2$ contamination was $\sim 5 \cdot 10^{-4}$ of the primary beam. The crystals were encapsulated in small Al containers and used directly in an ILL "orange" cryostat.

Our first experiments were at $T = 130\text{ K}$ (i.e., above the low-temperature phase transition reported in Ref. 5), and we found a situation compatible with the strain measured in Ref. 5. With the b axis vertical, the splitting of the peaks due to the orthorhombic twins is in the direction perpendicular to the scattering plane. The instrumental resolution is relatively poor in this direction so the integration usually, but not always, includes all peaks of both possible domains. To understand this better crystal no. 2 was used with $(hk0)$ reflections in the scattering plane. [Note that with the normal-beam method reflections out of this plane, up to $(hk2)$ in fact, can be measured.] The situation at the (800) and (080) reflections is illustrated in Fig. 1(a). First, $a < b$ so that the 2θ Bragg angles of (800) and (080) are different. Second, we find the line along which the two reflections lie coming, respectively, from twin A and twin B , is separated by $1.00 \pm 0.04^\circ$. The (660) reflection is single, so the common axis for the twinning is $\langle 110 \rangle$. The angle between $[100]_A$ and $[010]_B$ is then given by

$$\Psi = \arctan(a/b) - \arctan(b/a).$$

For the measured values of $a = 5.457(3)\text{ \AA}$ and $b = 5.546(3)\text{ \AA}$, $\Psi = 0.93 \pm 0.06$, and the strain

$$\epsilon = 2(b - a)/(b + a) = 1.6 \times 10^{-2}.$$

This is in excellent agreement with Ref. 5. The twinning

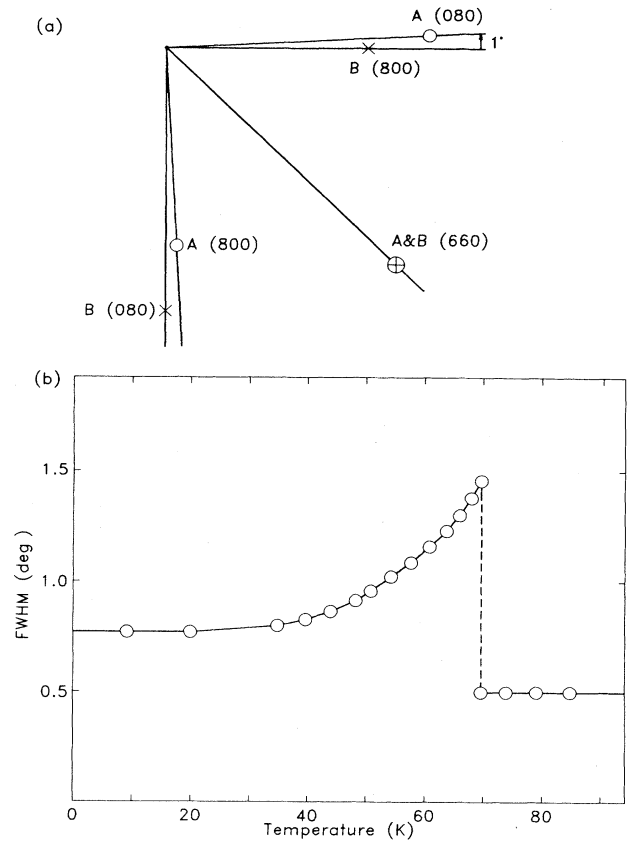


FIG. 1. (a) Schematic of reciprocal space at 130 K. A and B refer to the domains in the orthorhombic state. (b) Full width at half maximum (FWHM) of one of the $\langle 800 \rangle$ peaks as a function of temperature. Below $T_s = 70.0 \pm 0.5\text{ K}$ the peaks in La_2NiO_4 are single, but with a large FWHM, that gradually reduces down to $\sim 30\text{ K}$. Note that it is always greater than the experimental resolution which is 0.5° . (The reflection has $2\theta = 117.6^\circ$.)

direction is consistent³ with that found in La_2CuO_4 and also (perhaps by chance) with that in $\text{YBa}_2\text{Cu}_3\text{O}_7$. To understand the twin rule, reference should be made to Fig. 2 of Ref. 3, and the accompanying discussion.

Since the separation of the peaks increases with angle, the higher-order integrated intensities will be unreliable unless integration is over a very large volume in reciprocal space. Accordingly, we have not tried to perform a structural analysis with the data collected at 130 K. Some special sets of reflections will be reliable, e.g., those of the form (hhl) , and these are important in characterizing the low-temperature structure. Multiple-scattering effects also give rise to intensity at positions forbidden by the $Bmab$ space group. A particularly troublesome problem is the possibility of multiple scattering involving the nuclear and antiferromagnetic reflections (see below).

At $70.0 \pm 0.5\text{ K}$ a first-order phase transition occurs. Referring to Fig. 1(a) the individual peaks for $T > 70\text{ K}$ are resolution limited in their breadth. Thus, the (800) at $2\theta = 117.6^\circ$ has a full width at half maximum (FWHM) of

$\sim 0.5^\circ$. At the phase transition the two-peak structure, e.g., $A(080)+B(800)$, collapses to one peak. With our resolution we see no precursor of this and believe the transition is truly first order. Thus, $A(080)+B(800)$ are a single peak for $T < 70$ K, but the breadth of this peak is greater than the resolution. The FWHM versus temperature is shown in Fig. 1(b).

The experimental evidence presented below is consistent with the low-temperature phase being *tetragonal*. However, we must then explain the width of the (800)-type peak in Fig. 1(b) as an internal strain effect. Alternatively, if we postulate that the low-temperature phase is orthorhombic, then the width of the peak can give a limit on the quantity $|a-b| \leq 0.004$ at 10 K, which is less than the value of 0.007 given in Ref. 5, but differences between single crystals and powders are to be anticipated below such an abrupt transition.

B. Structural refinements

At 10 K a set of integrated intensities was measured from each crystal. The number of independent reflections was 165 for crystal no. 1 and 142 for crystal no. 2. Each independent reflection was the average of at least two, and usually four, symmetry related reflections.

The results of the least-squares refinements of the 307 independent reflections (both crystals) are given in Table I.

We may first start with the orthorhombic space-group *Bmab* (fifth column) of Table I. In this case it is necessary to take account of both twin domains, thus the (800) reflection will come from both $A(800)$ and $B(800)$ with possible unequal domain factors α_A and α_B . We have modified the least-squares routine to take account of this and find $\alpha_A = \alpha_B$, within statistics. Whereas the parameter values are reasonable in the *Bmab* refinement, the χ^2 and R values are high.

The second and third column give the result of refinements in the tetragonal space-group $P4_2/ncm$. Compared to the *Bmab* space group, there is a sharp reduction in both χ^2 and R , which is certainly significant. Adding anisotropic thermal temperature factors (third column) leads to a small improvement in the fit. We note that the Ni-O(1) distance is 1.951 Å and Ni-O(1') is 1.943 Å, whereas Ni-O(2) (along the c axis) is 2.219 Å, so that large B_{33} parameters for the oxygen and nickel atoms make physical sense. The similar distances in La_2CuO_4 are 1.894 and 2.428 Å, so the octahedron is significantly more distorted in the case of the Cu than in the Ni com-

TABLE I. Results of least-squares refinements of La_2NiO_4 data. η is the Becker-Coppens extinction parameter. The refinement of $\text{La}_{1.9}\text{Ba}_{0.1}\text{CuO}_4$ (powder data) is from Ref. 11. The third column gives the result of a refinement with anisotropic temperature factors, the first one being B_{11} , the second B_{33} . All cross terms are negligible. Scattering lengths were 0.824 for La, 1.03 for Ni, and 0.581 for O (all in 10^{-12} cm). Lattice parameters are given below the table.

Material	La_2NiO_4	La_2NiO_4	$\text{La}_{1.9}\text{Ba}_{0.1}\text{CuO}_4$	La_2NiO_4
Space group	$P4_2/ncm$	$P4_2/ncm$	$P4_2/ncm$	<i>Bmab</i>
T	10 K	10 K	15 K	10 K
η	0.029(3)	0.033(4)		0.035(14)
La (xxz)			La, Ba	La ($0yz$)
x or y	-0.0076(2)	-0.0075(2)	0.0040(3)	-0.0106(9)
z	0.3641(1)	0.3639(1)	0.3610(1)	0.3643(4)
B	0.21(3)	0.21(3)	0.1(1)	0.34(10)
		0.25(4)		
Ni (000)			Cu	Ni
B (\AA^2)	0.23(3)	0.17(3)	0.1(1)	0.34(10)
		0.36(4)		
O(1) ($\frac{1}{4}\frac{1}{4}z$)				
z	-0.0142(2)	-0.0146(2)	0.0079(4)	-0.0087(6)
B (\AA^2)	0.30(3)	0.23(4)	0.0(3)	0.42(11)
		0.43(5)		
O(1') ($\frac{3}{4}\frac{1}{4}0$)	($\frac{3}{4}\frac{1}{4}0$)	\rightarrow	\rightarrow	
B (\AA^2)	0.32(3)	0.26(4)	0.7(4)	
		0.54(7)		
O(2) (xxz)	(xxz)	\rightarrow	\rightarrow	O2 ($0yz$)
x or y	0.0296(3)	0.0296(4)	-0.0213(4)	0.039(2)
z	0.1769(1)	0.1769(2)	0.1824(2)	0.1770(5)
B (\AA^2)	0.47(3)	0.46(4)	0.6(1)	0.35(12)
		0.57(6)		
χ^2	43	40		582
R factor	6.4%	5.8%	3.1%	14.6%

La_2NiO_4 : $a = 5.502(3)$, $c = 12.504(11)$ Å

$\text{La}_{1.9}\text{Ba}_{0.1}\text{CuO}_4$: $a = 5.3559(2)$, $c = 13.2381(7)$

pound. Because the octahedron is less distorted than in La_2CuO_4 , the angle through which the octahedron is rocked¹⁰ on distorting from the HTT $I4/mmm$ structure is somewhat larger in the Ni compound. This may be determined as $\arctan(4zc/b)$, where z is the coordinate of O(1) or $\arctan(yb/zc)$ from the coordinates of O(2). For La_2NiO_4 these quantities are 7.6° from O(1) and 4.2° from O(2). For $\text{La}_{1.9}\text{Ba}_{0.1}\text{CuO}_4$ (Ref. 11) they are 4.2° from O(1) and 2.7° from O(2). That these angles are different when deduced from O(1) and O(2) indicates that the octahedra are not fixed (e.g., by the use of constraints in the refinement). Thus the refinements correspond not only to an elongation of the octahedra along its local fourfold axis, but also a small distortion of the faces. A slightly more physically meaningful approach might be to consider the octahedra as rigid entities.

In comparing parameters from various publications, the reader should be aware of the possibility of errors in the sign of $z(\text{O}(1))$ in some publications. This is discussed by Schultz *et al.*¹² We have also examined the stoichiometry by allowing the occupation parameters to vary in the refinement. The mean oxygen site occupation was determined as 1.005 ± 0.008 , and no improvement in R was obtained. Thus, the diffraction analysis confirms that the chemical preparation technique leads to stoichiometric samples.

A few comments may be made on the extinction and the relatively high values of χ^2 and R . Normally, for high-precision structural refinements we would use a crystal no larger than $\sim 5 \text{ mm}^3$. The use of a much larger (by a factor of ~ 10) crystal here was prompted by the very small signal anticipated in the polarized-beam study (Sec. IV). To our surprise the extinction in both crystals was a maximum of only $\sim 23\%$, on the strong (400) reflection. This made it possible to use the large crystal in the polarized-beam experiment, as extinction corrections of this magnitude can be reliable. We attribute the relatively low extinction in a crystal of this size to the strain effects already noted earlier, and demonstrated in Fig. 1(b). However, these large crystals are bigger than usually used on $D15$, which may result in failure to correctly integrate the reflections leading to equivalences somewhat poorer than usually obtained on this diffractometer. Given these caveats, we believe an R factor of 6.0% represents a good fit.

C. Low-temperature tetragonal phase

The low-temperature tetragonal (LTT) phase¹¹ is a very interesting modification of the LTO phase, in which the buckling of the octahedra is about alternate [110] axes rather than about a [010] axis in the LTO phase. This modification has been proposed and discussed in detail by Axe *et al.*¹¹ In the LTT phase with $P4_2/nm$ new reflections should appear that are systematically absent with LTO ($Bmab$). In Fig. 2 we show the absolute intensity (normalized by using scale factors from the least-squares refinements) of the $(11l)$ l -even reflections as measured at $T=130$ and 10 K. Because the twinning is about the $\langle 110 \rangle$ axes the $(11l)$ reflections are single peaks even at 130 K, so reliable comparisons of the inten-

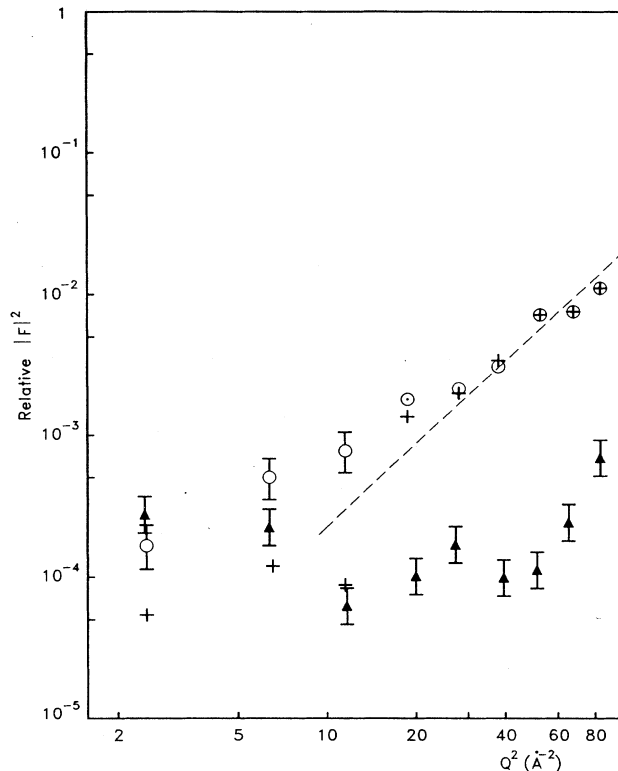


FIG. 2. Variation of the $(11l)$ l -even reflections as a function of Q^2 for 130 K (solid triangles) and 10 K (open circles). These reflections should be systematically absent in the $Bmab$ phase because $h+l$ -odd. The level of multiple scattering and $\lambda/2$ is $\sim 10^4$ (the strongest Bragg reflection is 1 on this scale). The calculated intensities in the $P4_2/nm$ phase are given as crosses. The dashed line gives the Q^2 -dependence slope.

sities at 130 and 10 K can be made. In the LTO phase these reflections should be systematically absent, and we find values around the 10^{-4} level, which is approximately that of the multiple scattering and $\lambda/2$ contamination. However, in the LTT phase the crosses give the calculated values, which are in excellent accord with the observed values (circles). Because the difference between the two phases is a small displacement of atoms, we anticipate the new intensities to vary as some higher power of Q ; this is indeed found to be the case. In this kind of analysis single-crystal data are much more powerful than data from a polycrystalline sample.

Another space group that has been suggested for the low-temperature phase is $Pccn$. However, as compared to $P4_2/nm$ there are no additional new classes of reflections. There are, of course, additional atomic parameters presents in $Pccn$, but since we do not observe any splitting of the reflections we do not feel justified in adding further parameters to our refinement.

IV. ANTIFERROMAGNETISM

The antiferromagnetic (AF) structure of La_2NiO_4 is well known.¹³ In the LTO phase the spins are parallel to

[100] and the propagation direction is also [100]. This gives rise to reflections of the form h even, k and l odd, or h odd, k and l even. In a single domain (LTO) phase the intensity of the $(h00)$ reflections would be zero because of the q^2 magnetic interaction vector. However, the $(100)_A$ is close to the $(010)_B$ so intensity is present at these points. We can see, however, that at $T=130$ K only domain B contributes to the $(h00)$ reflections and domain A to $(0k0)$ reflections because these peaks are single, whereas the nuclear peaks are double. At low temperature in the LTT phase the magnetic *symmetry* is still orthorhombic so magnetic domains will be present in this phase as well. The susceptibility measurements on a crystal from the same boule as the crystals used in the neutron study are reported in Ref. 8. The antiferromagnetic transition¹⁴ is at 650 K, and a small discontinuity is seen at 70 K. We find no change in the magnetic reflections at T_s . Rodriguez-Carvajal *et al.*⁵ also report no change in the magnetic intensities at the 70 K transition. A recent study¹⁵ of La_2CoO_4 has shown that a change in the antiferromagnetic structure occurs at T_s in the Co compound.

We have not checked T_N on our sample with neutrons but the AF order is still present at 300 K, and little changed from 10 K. This is consistent with a T_N above ~ 600 K. It is remarkable how rapidly T_N decreases as one moves away from stoichiometry.¹³ The appearance of additional magnetic peaks not permitted by either the LTO or LTT phase greatly increases the possibility for multiple scattering. This has been discussed at length by Freltoff *et al.*¹⁶ in their study of La_2CuO_4 . Since we have used a short neutron wavelength these problems are severe. The strongest magnetic reflection, the (011) has an intensity of 4.4×10^{-3} . Only one domain type, i.e., 50% of the crystal volume, contributes to each AF reflection. In principle, we could extract a AF form factor as in Ref. 16, but this would require more care in eliminating or understanding the multiple effects. We have not done this, but have used the two strongest reflections (011) and (013) from the two crystals to obtain the ordered moment in the AF state. We obtain values of 1.67 and $1.57\mu_B$, each $\pm 0.08\mu_B$, respectively. This uses a Ni^{2+} form factor. The Ni AF moment may then be taken as $1.62 \pm 0.05\mu_B$ at 10 K in stoichiometric La_2NiO_4 .

In La_2CoO_4 the spin direction is reported to change at the LTO \rightarrow LTT transition, which is at 135 K. The fact that we see no change in the magnetic intensities at 70 K is a strong indication that the magnetic structure stays the same, but it is not conclusive. In the simplest model we have two domains in the tetragonal phase, one with the moments parallel to [100], the other with them parallel to [010]. However, since [100] and [010] have the same d space in the tetragonal phase we cannot separate these domain populations (this is possible in the orthorhombic phase), and it is just as likely that the two components are combined in a $2k$ magnetic structure.¹⁷ In this case, the spins would lie along the $\langle 110 \rangle$ axes in the LTT phase. We cannot exclude such a complex magnetic structure in the LTT phase. However, any canting of the spins towards the c axis must be very small.

V. POLARIZED-NEUTRON MEASUREMENTS

The objective of this experiment was to examine in detail the nature of the wave functions of the unpaired electrons in La_2NiO_4 when a magnetic field is applied. A frequently postulated feature¹⁸ of the oxides is that the d_{z^2} states, whose lobes point along the c axis, form bonding and antibonding states far removed from E_F , and that the principal bonding states are formed by a mixing of the p_x and p_y orbitals of O(1) [and O(1') in the LTT phase] and the $d_{x^2-y^2}$ states of Ni^{2+} (or Cu^{2+} in the copper compound). These states are supposed to form a broad band with E_F lying in this band, and this gives the metallic nature of these systems. When a magnetic field is applied (either an internal exchange field or an external applied field) the spin-up and spin-down states are split in energy, with the spin-up band lowered. In this *metallic* model the spin density (or magnetization density if we suppose that there is a small orbital moment) is representative of the states near E_F . It is the spatial extent of this spin density that is measured in our experiment.

The technique is relatively simple.¹⁹ A beam of polarized neutrons from the ILL reactor hot source is monochromatized and simultaneously polarized by a Heusler alloy single crystal. We have used a wavelength of 0.843 Å for the major data collection, but wavelengths of 0.711 and 0.545 Å were used to check the extinction corrections. Suitable filters reduced the $\lambda/2$ component to less than 6×10^{-3} , allowing accurate $\lambda/2$ corrections to be made. This beam of polarized neutrons, initially polarized with $\mathbf{P} \parallel \mathbf{H}$ is then Bragg diffracted from the sample. The intensity of this diffracted beam is proportional to $(N+M)^2$ where N and M are the nuclear and magnetic structure factors, respectively. It should be stressed that the moment contributing to M is that aligned by the applied field. These measurements are done at nuclear Bragg peaks. The polarization of the incident neutrons is then changed to $\mathbf{P} \parallel -\mathbf{H}$ and the intensity is now proportional to $(N-M)^2$. The experiment consists of measuring the ratio of the two intensities, the so-called flipping ratio

$$R = (N+M)^2 / (N-M)^2,$$

from which the value of $\gamma = M/N$ can immediately be deduced. $N(hkl)$ are the nuclear structure factors, which are accurately known from the earlier part of this paper, so that we can immediately determine $M(hkl)$, the quantity of interest. A Fourier transform of $M(hkl)$ will give us the magnetization density.

A. Measurements and corrections

We studied a total of 18 reflections from crystal no. 1 with the field oriented within 5° of the b axis. All data were taken at 5 K with an applied field of 4.6 T. The details are given in Table II. Since these are all F -type nuclear reflections (h, k, l either all even or all odd), they are relatively strong. We would not expect these $N(hkl)$ values to be very sensitive to the small atomic displacements discussed in relation to the space-groups $P4_2/ncm$

TABLE II. Results of polarized-neutron study of La_2NiO_4 at $T=5$ K, $H=4.6$ T, $\mathbf{H}\parallel\mathbf{b}$. All numbers refer to 1 formula unit. N is the nuclear structure factor, γ (column 4) is that with $\lambda=0.843$ Å, N_{La} is the structure factor of just the La atom with a sign relative to that of the Ni contribution, M_D is the diamagnetic correction, M_0 is the observed magnetic structure factor, and M_c is the calculated. (1) and (2) both use Ni^{2+} form factors. In (1) $\mu_{\text{Ni}}=5.86(22)$ $m\mu_B$, $\mu_{\text{La}}=0$, whereas in (2), $\mu_{\text{Ni}}=5.98(13)$, $\mu_{\text{La}}=0.95(9)$ $m\mu_B$. When comparing M_0 and M_c , $\chi^2=4.7$ for (1), and 1.6 for (2). Standard deviations in parenthesis refer to least significant digit.

hkl	$\frac{\sin\theta}{\lambda}$ (Å ⁻¹)	$ N $	γ $\times 10^4$	N_{La}	M_D ($m\mu_B$)	M_0 ($m\mu_B$)	(1)	(2)
							M_c ($m\mu_B$)	M_c ($m\mu_B$)
2 0 0	0.184	2.565	4.9(6)	1.63	-0.37	5.6(4)	4.45	5.93
4 0 0	0.367	4.503	1.4(4)	1.55	-0.15	2.8(6)	2.20	2.86
1 1 1	0.136	0.441	21.0(26)	-1.08	0.16	3.6(4)	5.02	4.09
3 1 1	0.293	0.377	13.0(40)	-1.04	0.06	1.6(4)	3.05	2.53
0 0 2	0.079	1.246	10.7(8)	0.23	-0.03	5.0(3)	5.55	5.43
2 0 2	0.200	0.989	10.7(12)	-0.22	-0.03	4.0(4)	4.25	4.15
4 0 2	0.375	1.403	4.9(11)	-0.21	-0.02	2.5(5)	4.13	4.09
1 1 3	0.176	1.304	9.3(11)	1.37	-0.33	5.4(5)	4.55	5.84
3 1 3	0.313	1.633	5.2(15)	1.33	-0.17	3.3(5)	2.81	3.53
0 0 4	0.158	0.256	22.9(34)	-1.58	0.25	3.6(4)	4.75	3.43
2 0 4	0.242	1.921	5.3(7)	-1.56	0.16	3.6(4)	3.67	2.70
1 1 5	0.236	2.528	3.7(6)	0.70	-0.16	4.3(4)	3.75	4.33
3 1 5	0.351	2.371	3.7(6)	0.68	-0.09	3.7(4)	2.38	2.71
0 0 6	0.237	0.760	2.8(4)	0.65	-0.15	4.3(5)	3.75	4.30
2 0 6	0.300	1.572	5.6(9)	0.64	-0.11	3.6(4)	2.95	3.38
1 1 7	0.306	0.462	11.6(28)	-1.54	0.10	2.6(4)	2.88	2.15
0 0 8	0.316	2.404	4.6(6)	1.38	-0.17	4.1(5)	2.78	3.50
2 0 8	0.366	0.533	12.0(36)	1.35	-0.13	3.3(6)	2.22	2.80

and B_{mab} , and indeed this is the case. Furthermore, we are working at small Q ($\sin\theta/\lambda < 0.4$ Å⁻¹). Each R value was measured from at least two, and usually four, equivalent reflections. Fifteen of the reflections were measured also at 0.711 Å and six at 0.545 Å. The γ values are small (those for $\lambda=0.843$ Å are given in Table II) so that the R values, where $R \sim 1+4\gamma$, are close to unity. This requires long counting times and large crystals. The extinction corrections were made on the basis of the least-squares refinement described in Sec. III. The final $M_0(hkl)$ is a mean of all values and the sigma represents the true sigma calculated from the distribution of measurements. No values were rejected. Corrections for incomplete polarization of the incident neutrons were made in each case and are known to better than 2%. Other corrections include spin-orbit scattering,²⁰ diamagnetism,²¹ and higher-order contamination. The spin-orbit term is negligible.

The diamagnetism of the core electrons in La_2NiO_4 is -1.0×10^{-4} emu/mol. The extent to which these core electrons are observed with neutrons is well known, and the resulting form factor may be calculated exactly. This contribution is listed as M_D in Table II. As expected, the dominant contribution is from the La core electrons, and we note in Table II that the sign of M_D is almost always opposite to that of N_{La} , the structure factor of the La atom. The largest diamagnetic correction is ~ 0.4 $m\mu_B$, which is about the size of the average error bar, see column labeled M_0 in Table II.

Corrections for second-order wavelength contamination are only important (i.e., $> 10\%$) for the (004), (117), and (208) reflections. In the case of the (004), the $\lambda/2$ contamination arises from scattering from the (008) reflection, which is ~ 60 times more intense than the (004). We have used the observed ratio of (004) to (008) from our earlier structure refinement to obtain a $\lambda/2$ correction of 28%.

B. Magnetic form factor

The simplest way to illustrate the variation of $M_0(hkl)$ is to plot these values versus $\sin\theta/\lambda$. This is done in Fig. 3. If all the magnetization density was associated with a spherically symmetric Ni atom we should expect all points to lie on a smooth curve, which they do not. We have drawn a Ni^{2+} form factor as the dashed curve that extrapolates to 6.15 ± 0.20 $m\mu_B$ per formula unit. This corresponds to a susceptibility of $(0.75 \pm 0.02) \times 10^{-3}$ emu/mol. The most pertinent question to ask about the data of Fig. 3 is whether the deviations of the data from the smooth curve are significant.

C. Fourier transform

As is well known the Fourier transform of the form factor gives the magnetization density in the unit cell. However, in our case the data set is incomplete, so that a direct Fourier transform is unreliable. Instead, we first calculate the magnetic structure factor for each reflection

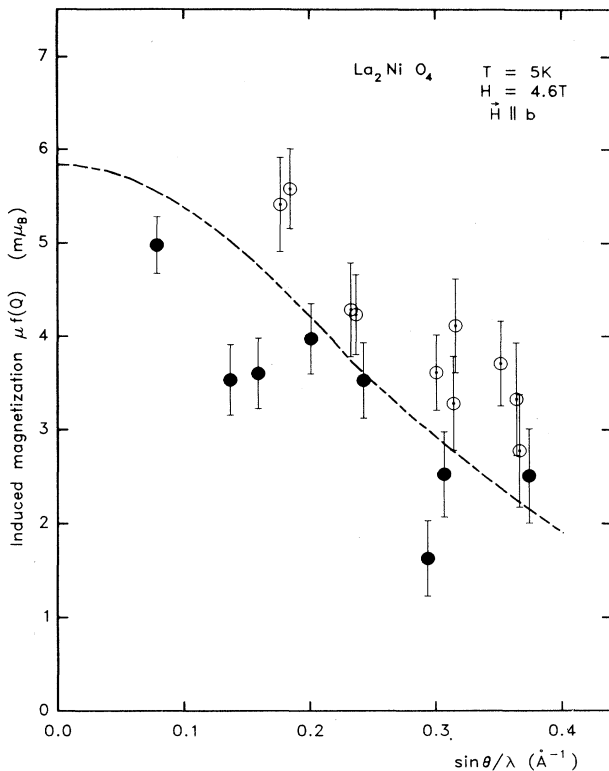


FIG. 3. The form factor at 10 K of the induced spin density in the antiferromagnetic state of La_2NiO_4 . The open (solid) circles correspond to those in which the Ni and La contributions are parallel (antiparallel), see the text. The dashed line is a Ni^{2+} form factor giving a susceptibility (intercept at $\sin\theta/\lambda=0$) of $5.85 m\mu_B$ for the applied field of 4.6 T. ($Q = 4\pi \sin\theta/\lambda$.)

$M_c(hkl)$ based on the assumption that all the moment is at the Ni site and that the spatial extent corresponds to a spherically symmetric Ni^{2+} form factor. We then form the difference coefficient $[M_0(hkl) - M_c(hkl)]$ and perform the Fourier transform with these difference coefficients. The resulting density is averaged over a cube of edge 0.5 \AA to further decrease errors due to an incomplete data set. The first thing we observe is that there is no significant difference density in the Ni-O planes, i.e., in the $(xy0)$ and $(xy\frac{1}{2})$ sections of the structure. What this implies is that our induced spin density measurements in La_2NiO_4 have failed to find any evidence for a preferential population of $d_{x^2-y^2}$ Ni^{2+} orbital, nor any strong overlap effects between the $d_{x^2-y^2}$ Ni and the oxygen $2p_x$ or $2p_y$ states. The Ni spin density in these planes appears circularly symmetric. This corresponds to a half-filled subshell of, e.g., symmetry, with the two electrons forming the high-spin $S = 1$ state.

On the other hand, we do find evidence for unusual effects along the c axis. The relevant section of the spin density is shown in Fig. 4. Two features are immediately obvious. There is a small susceptibility associated with the La site, and there is evidence for overlap effects between the Ni and O(2) atoms. The susceptibility associated with the La atom is the dominant feature of this map, and is so unusual that we shall discuss some qualitative

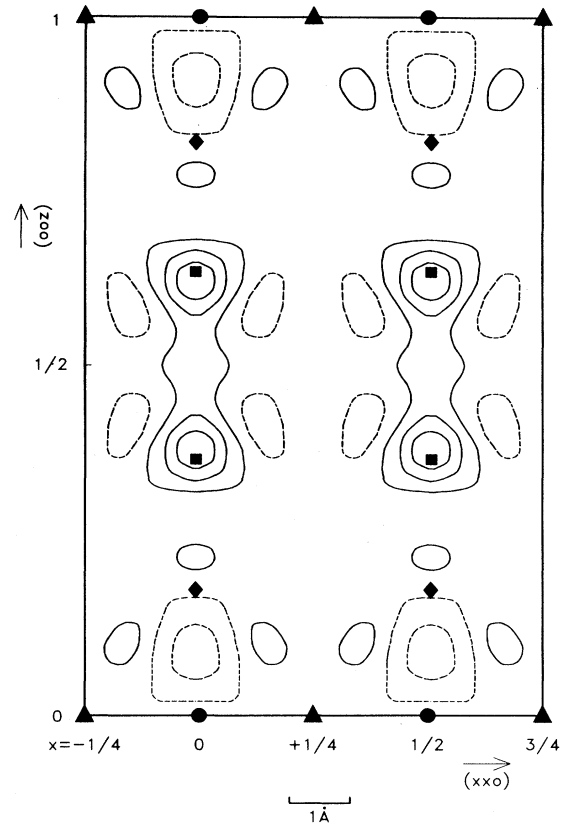


FIG. 4. Difference ($M_0 - M_c$) Fourier in La_2NiO_4 at 10 K. The significance level (deduced from the experimental uncertainties) is ~ 1 contour. This cross section contains all atoms in the structure. The difference Fourier has been averaged over a cube of edge 0.5 \AA . Solid (dashed) contours correspond to positive (negative) regions in the difference map. The atom symbols are \blacksquare , La; \bullet , Ni; \blacktriangle , oxygen O(1) and O(1); \square , O(2).

aspect of this result before proceeding with the modeling of the difference spin density. This susceptibility is approximately $0.8 m\mu_B/\text{La}$ atom divided by the field of 4.6 T, i.e., $+(1.0 \times 10^{-4}) \text{ emu/La}$ atom. This quantity, which is $\sim 16\%$ of the susceptibility at the Ni site, will clearly interfere either constructively or destructively with the signal from the Ni depending on the phase relationship between La and Ni in a given reflection (hkl). La_2NiO_4 , of course, is centrosymmetric so we may just consider whether the La contributions add or subtract from the Ni moment. As shown in Fig. 3 the open (solid) circles have La adding to the Ni contribution, and the solid circles involve a subtraction. We should emphasize that this argument comes solely from considering the crystal structure, nor is it quantitative in the sense that the amounts to be added or subtracted are not equal for all (hkl). However, the excellent correlation of open (solid) circles above (below) the Ni^{2+} form factor, is clear qualitative proof that the major asymmetries in the form factor of Fig. 3 arise from a contribution at the La site, and that it must be parallel to the Ni contribution.

D. Modeling the lanthanum susceptibility

To obtain a more quantitative agreement between calculated and observed magnetic structure factors we have performed a least-squares analysis involving the quantities μ_{Ni} and μ_{La} . We should emphasize again that as the experiment was carried out in the antiferromagnetic state, the magnetic structure factors measured are due to that part of the moment which is pulled parallel to the field direction (b) by an applied field of 4.6 T. The moments to be fitted for nickel and lanthanum are really susceptibilities and their relative magnitudes will not necessarily reflect the ratio of moments present in the antiferromagnetic structure. Before a least-squares fit to the moment values can be carried out we need to model the spatial extent of the atomic moment distributions, i.e., the form factors f_{Ni} and f_{La} . For f_{Ni} the Ni^{2+} form factor was used. Our first expectation was that f_{La} would have a strong $5d$ -like character, but it is well known that a $5d$ free-atom form factor falls very rapidly²² with $\sin\theta/\lambda$, having essentially zero amplitude by $\sin\theta/\lambda \approx 0.2 \text{ \AA}^{-1}$. However, we can see from Fig. 3 that interference effects are still present between $(\mu f)_{\text{Ni}}$ and $(\mu f)_{\text{La}}$ at $\sin\theta/\lambda \approx 0.35 \text{ \AA}^{-1}$ so that a free-ion $5d$ form factor is inappropriate. An attempt was made to determine the form factor experimentally using a Fourier integration method,²³ but this proved unsatisfactory as, due to the limited data available, series termination effects seriously perturb the density included in the integration sphere around the lanthanum atom. The qualitative results of this analysis and that of the previous section suggest that the spatial extent of the La spin density can be approximately modeled by a Ce $4f$ form factor, and we have used this for the least-squares fit. We cannot, of course, exclude the possibility that both $4f$ - and $5d$ -like electrons contribute to the positive susceptibility at the La site. There may also be a significant change from the free-atom wave functions; for example, an apparent compaction could be the result of overlap between La $5d$ electrons of positive spin and s and p electrons of opposite polarization from the ligand oxygen atoms.

Using such an f_{La} function we find the best fits are as follows:

μ_{Ni}	5.86(22) $m\mu_B$	5.98(13) $m\mu_B$
μ_{La}	0	0.95(9) $m\mu_B$
χ^2	4.7	1.6
χ_M	$0.71(3) \times 10^{-3}$ emu/mol	$0.96(2) \times 10^{-3}$ emu/mol

The corresponding values for M_c are given in Table II, and it is immediately clear that the second column of M_c gives a far better fit ($\chi^2=1.6$) than the first ($\chi^2=4.7$). The total susceptibility χ_M as deduced from the neutron experiments $0.96(2) \times 10^{-3}$ emu/mol, is in excellent agreement with the value of 0.95×10^{-3} measured in the bulk magnetization.⁸

We have then recalculated the difference map with the M_c coefficients of the final column of Table II. As expected, the positive contours at the La site are now absent, but the pattern of negative contours between the Ni and O(2) atoms remains. This negative oxygen contribu-

tion supports the suggestion that it is cancellation between oxygen and lanthanum which sharpens the $5d$ form factor. However, these contour levels are at the limit of our significance and with a $\chi^2=1.6$ in the above model we do not feel justified in modeling further.

VI. DISCUSSION

The first part of this paper describes the structural phase transition at 70 K in stoichiometric La_2NiO_4 . Above 70 K the material has the space-group $Bmab$ (orthorhombic) with the twin axis $\langle 110 \rangle$. Below 70 K we believe the orthorhombic structure transforms to a low-temperature tetragonal form with symmetry $P4_2/ncm$. It is also possible that the low-temperature modification has space-group (orthorhombic) $Pccn$ but with a strain $2(a-b)/(a+b) \leq 4 \cdot 10^{-3}$. Higher resolution x-ray or neutron measurements could answer this question. We note that the systematic absences are the same for $P4_2/ncm$ and $Pccn$.

We find the antiferromagnetic moment to be $1.62(5)\mu_B/\text{Ni}$ atom. Our sample is antiferromagnetic at room temperature; for stoichiometric La_2NiO_4 $T_N \approx 650$ K. The magnetic structure¹³ consists of [100] planes of parallel Ni moments with the spins parallel to [100]. No changes are observed at 70 K.

In the second part of the experiment a 4.6 T field has been applied parallel to [010] (or equivalently [100] in the tetragonal $P4_2/ncm$ representation) and the spatial extent of the small *induced* magnetic moment measured with polarized neutrons. Our original hope had been to compare the results of La_2NiO_4 with those (then in progress) on La_2CuO_4 (Ref. 6). However, these latter measurements were not made with sufficient precision for such a comparison. The experiment on La_2CuO_4 is more difficult than the present one because the susceptibility is ~ 4 times smaller. A further aim was to examine any covalency between the Ni^{2+} $d_{x^2-y^2}$ orbitals and the p_x and p_y states of the planar oxygen atoms. We find none; indeed the Ni^{2+} is almost spherically symmetric, indicating an equal population of $d_{x^2-y^2}$ and d_{z^2} , and no significant covalency in the Ni-O plane.

However, there is an unusual feature to the spin density. We find a *positive susceptibility* at the La site. Harmon²⁴ and Spzunar *et al.*²⁵ have suggested that this arises because of mixing between the La and O states and the consequent lowering of the energy of the La $5d$ states. If there is minority spin density in s or p states associated with the oxygen atoms, then overlap effects may account for the observation that the spin density at the La site ($\sim 16\%$ of that observed on a Ni atom) is considerably more contracted than a free-atom $5d$ state. The observation of a small negative spin density at the O₁ site adds some weight to this argument. A possible contribution from the nominally unoccupied La $4f$ states must also be considered if sufficient hybridization occurs. It seems probable that the La spin density is directly induced by the applied field, and as such reflects the susceptibility of electron states at the Fermi surface; this is in contrast to the nickel and any associated oxygen spin density which

arises from tilting of the local moments present in the antiferromagnetic states towards the applied field direction. It is difficult for us to associate this feature with any superconducting properties of either La_2CuO_4 or La_2NiO_4 . If it can be reproduced by detailed band-structure calculations, now in progress,^{24,25} then it will give considerable confidence in those calculations.

It is known that substitution of rare-earth atoms for lanthanum in La_2CuO_4 strongly depresses the superconductivity, (solubility considerations limit the amount of substitution), whereas similar substitution of trivalent rare earths for yttrium in $\text{YBa}_2\text{Cu}_2\text{O}_7$ has essentially no effect upon T_c . Polarized-neutron experiments on the 1-2-3 system²⁶ give no evidence of susceptibility at the Y site indicating a closed-shell Y configuration with no Y-O interaction. Our results for La_2NiO_4 , on the other hand, show that in this compound there is a path, via the La-O hybridization, for direct interaction between the superconducting sheets. This may explain why any unpaired

4f electrons substituted at the La site have such a strong depressive effect on T_c .

A more interesting question is what effect divalent Sr^{2+} or Ba^{2+} substitution will have on the La susceptibility found in our measurements. We shall attempt to answer this question with future experiments.

ACKNOWLEDGMENTS

One of us (G.H.L.) would like to thank John Axe for sharing his ideas about the low-temperature tetragonal structure, which seems to apply so well to La_2NiO_4 . We thank Juan Rodriguez-Carvajal and Jean Pannetier for sharing their results on polycrystalline samples, Bruce Harmon and Costa Stassis for discussion, and Jean Rebizant for help in encapsulating the samples. Work at Purdue is sponsored by the National Science Foundation.

- ¹J. G. Bednorz and K. A. Muller, *Z. Phys. B* **64**, 189 (1986).
- ²J. D. Jorgensen, H. B. Schüttler, D. G. Hinks, D. W. Capone, K. Zhang, M. B. Brodsky, and D. J. Scalapino, *Phys. Rev. Lett.* **58**, 1024 (1987); D. McK. Paul, G. Balakrishnan, N. R. Bernhoeft, W. I. F. David, and W. T. A. Harrison, *ibid.* **58**, 1976 (1987).
- ³J. M. Delgado, R. K. McMullen, G. Diaz de Delgado, B. J. Wuensch, P. J. Picone, H. P. Jensen, and D. R. Gabbe, *Phys. Rev. B* **37**, 9343 (1988).
- ⁴J. Fontcuberta, G. Langworth, and J. B. Goodenough, *Phys. Rev. B* **30**, 6320 (1984).
- ⁵J. Rodriguez-Carvajal, J. L. Martinez, J. Pannetier, and R. Saez-Puche, *Phys. Rev. B* **38**, 7148 (1988).
- ⁶C. Stassis, B. N. Harmon, T. Freltoft, G. Shirane, S. K. Sinha, K. Yamada, T. Endoh, Y. Hidaka, and T. Murakami, *Phys. Rev. B* **38**, 9291 (1988).
- ⁷Z. Kakol, J. Spalek, and J. M. Honig, *Solid State Chem.* **79**, 288 (1989).
- ⁸Z. Kakol, J. Spalek, and J. M. Honig, *Solid State Commun.* (to be published).
- ⁹D. J. Buttrey, H. R. Harrison, J. M. Honig, and R. R. Schartman, *J. Solid State Chem.* **54**, 407 (1984).
- ¹⁰P. Boni, J. D. Axe, G. Shirane, R. G. Birgeneau, D. R. Gabbe, H. P. Jensen, M. A. Kastner, C. J. Peters, P. J. Picone, and R. R. Thurston, *Phys. Rev. B* **38**, 185 (1988).
- ¹¹J. D. Axe, D. E. Cox, K. Mohanty, H. Moudden, A. R. Moodenbaugh, Y. Xu, and T. R. Thurston, *IBM J. Res. Dev.* (to be published); J. D. Axe, A. H. Moudden, D. Hohlwelm, D. E. Cox, K. M. Mohanty, A. R. Moodenbaugh, and Y. Xu, *Phys. Rev. Lett.* **62**, 2751 (1989).
- ¹²A. J. Schultz, C. K. Loong, J. Z. Liu, W. K. Kwok, G. W. Crabtree, and D. J. Lam, *Physica C* **157**, 301 (1989).
- ¹³G. Aeppli and D. J. Buttrey, *Phys. Rev. Lett.* **61**, 203 (1988).
- ¹⁴R. R. Schartman and J. M. Honig, *J. Solid State Chem.* (to be published); D. J. Buttrey, J. M. Honig, and C. N. R. Rao, *ibid.* **64**, 287 (1986).
- ¹⁵K. Yamada, M. Matouda, Y. Endoh, B. Keimer, R. J. Birgeneau, S. Onodera, J. Misusaki, T. Matsuura, and G. Shirane, *Phys. Rev. B* **39**, 2336 (1989).
- ¹⁶T. Freltoft, G. Shirane, S. Mitsuda, J. P. Remeika, and A. S. Cooper, *Phys. Rev. B* **37**, 137 (1988).
- ¹⁷J. Rossat-Mignod, P. Burlet, S. Quezel, and O. Vogt, *Physica B* **102**, 237 (1980).
- ¹⁸J. A. Wilson, *J. Phys. (London) C* **21**, 2067 (1988).
- ¹⁹R. Nathans, C. G. Shull, G. Shirane, and A. Andresen, *J. Phys. Chem. Solids* **10**, 138 (1959); P. J. Brown, J. B. Forsyth, and R. Mason, *Philos. Trans. R. Soc. London, Ser. B* **290**, 481 (1980).
- ²⁰C. G. Shull, *Phys. Rev. Lett.* **10**, 297 (1963); G. P. Felcher and S. W. Peterson, *Acta Crystallogr. A* **31**, 76 (1975).
- ²¹C. Stassis, *Phys. Rev. Lett.* **24**, 1415 (1970).
- ²²T. O. Brun and G. H. Lander, *Phys. Rev. Lett.* **23**, 1295 (1969); R. M. Moon, W. C. Koehler, J. W. Cable, and H. R. Child, *Phys. Rev. B* **5**, 997 (1972).
- ²³P. J. Brown and C. Wilkinson, *Acta Crystallogr.* **18**, 398 (1965).
- ²⁴B. Harmon (private communication).
- ²⁵B. Szpunar, V. H. Smith, and J. Spalek, *Physica C* (to be published).
- ²⁶B. Gillon, D. Petitgrand, A. Delapalme, P. Radhakrishna, and G. Collin, *Physica B* **156-157**, 851 (1989).